

FEM model for real-time guide wire simulation in vasculature

Zhang Qiukui¹ Pascal Haigron² Luo Limin¹ Shu Huazhong¹

(¹ Laboratory of Image Science and Technology, Southeast University, Nanjing 210096, China)

(² Laboratory of Treatment of Signal and Image, University of Rennes 1, Rennes 35042, France)

Abstract: A model suitable for describing the mechanical response of thin elastic objects is proposed to simulate the deformation of guide wires in minimally invasive interventions. The main objective of this simulation is to provide doctors an opportunity to rehearse the surgery and select an optimal operation plan before the real surgery. In this model the guide wire is discretized with the multi-body representation and its elastic energy derived from elastic theory is a polynomial function of the nodal displacements. The vascular structure is represented by a tetrahedron mesh extended from the triangular mesh of the artery, which can be extracted from the patient's CT image data. The model applies the energy decline process of the conjugate gradient method to the deformation simulation of the guide wire. Experimental results show that the polynomial relationship between elastic energy and nodal displacements tremendously simplifies the evaluation of the conjugate gradient method and significantly improves the model's efficiency. Compared with models depending on an explicit scheme for evaluation, the new model is not only non-conditionally stable but also more efficient. The model can be applied to the real-time simulation of guide wire in a vascular structure.

Key words: deformable model; finite element method; real-time simulation; guide wire

Minimally invasive surgery has radically changed traditional surgical techniques. It has many advantages over conventional surgery in many respects. But minimally invasive interventions require strict training of the interventionalist. In these interventions, a guide wire needs to be manipulated under fluoroscopic guidance. A novice surgeon must practice for a long time to obtain such ability. For this reason, there is a great interest in developing guide wire simulation software to provide a comprehensive training system as well as a useful means to obtain pre-operative knowledge of the undergoing intervention.

Many techniques have been investigated by different groups to simulate the deformation of thin solid objects. A spline animated by continuous mechanics with the Lagrangian formalism was proposed by Lenoir et al.^[1] LeDuc introduced a model with "home springs" derived from the mass-spring model^[2] in which springs are connected along the thread. The fact that strength, bending and torsion behaviors are not considered makes them difficult to apply in our situation. Physically based models were also proposed to introduce these kinds of behavior through different representations. Konings et al.^[3] proposed to minimize only the bending energy of the guide wire-artery wall system by a discrete method. Cotin et

al.^[4] defined a model of guide wire and a patient-specific artery representation using an incremental FEM with substructures analysis. Guilloux et al.^[5] introduced a virtual environment dedicated to the simulation of the guide wire navigation in the vasculature considering its physical properties. Cao et al.^[6] proposed a Cosserat rod element approach for three-dimensional nonlinear dynamics of slender structures and Pai^[7] introduced the Cosserat model into the interactive simulation of thin solids.

Unfortunately, the existing models based on spring meshes or continuum-mechanics are either inaccurate or inefficient for interactive simulation. None of the techniques for physically based modeling is well suited for the task of real-time simulation of the guide wire inside arteries. The objective of this paper is to develop an efficient and robust deformable model based on the elastic theory and the FEM for the real-time simulation of the guide wire inside arteries.

1 Guide Wire's FEM model

Following the multi-body representation^[8] the guide wire is discretized as a chain of small and elastic cylindrical segments. Each one is connected to its neighbors at joints known as nodes. The small cylindrical segment is also called the beam element. Two successive beam elements form one bend element (see Fig. 1). With these elements we can evaluate the deformation energy and the elastic force of the structure.

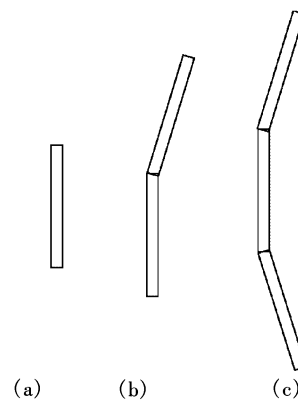


Fig. 1 Different kinds of elements and an element chain.
(a) Beam element; (b) Bend element; (c) Wire model

1.1 Stretch modeling

The beam element works as a stiff spring. When stretched or compressed, it generates elastic forces on its nodes. The force is in the direction of the axis of the beam element and its magnitude is usually decided by Hooke's law:

$$f_s = \bar{k}_s (r - r_0) \quad (1)$$

Received 2007-08-31.

Biographies: Zhang Qiukui (1971—), male, graduate; Luo Limin (corresponding author), male, doctor, professor, luo.list@seu.edu.cn.

Citation: Zhang Qiukui, Pascal Haigron, Luo Limin, et al. FEM model for real-time guide wire simulation in vasculature[J]. Journal of Southeast University (English Edition), 2008, 24(1): 50 – 54.

where r and r_0 are the current and the original lengths of the beam element, respectively. To simplify the expression, we use the following vector and matrix symbols:

$$\mathbf{x}_s = \begin{Bmatrix} \mathbf{x}_0 \\ \mathbf{x}_1 \end{Bmatrix}, \quad \mathbf{f}_s = \begin{Bmatrix} \mathbf{f}_s^0 \\ \mathbf{f}_s^1 \end{Bmatrix}, \quad \mathbf{B}_s = [-\mathbf{I} \quad \mathbf{I}] \quad (2)$$

where \mathbf{x}_0 and \mathbf{x}_1 are the three-dimensional position vectors of the two nodes of the element, \mathbf{f}_s^0 and \mathbf{f}_s^1 are the elastic forces applied to the two nodes, \mathbf{I} is a 3×3 identity matrix, \mathbf{x}_s and \mathbf{f}_s are six-dimensional vectors and \mathbf{B}_s is a 3×6 constant matrix. We use the following vector equation to evaluate the force vector:

$$\mathbf{f}_s = \frac{\bar{k}_s(\sqrt{\mathbf{x}_s^T \mathbf{B}_s^T \mathbf{B}_s \mathbf{x}_s} - r_0) \mathbf{B}_s^T \mathbf{B}_s \mathbf{x}_s}{\sqrt{\mathbf{x}_s^T \mathbf{B}_s^T \mathbf{B}_s \mathbf{x}_s}} \quad (3)$$

Because the square root appears in the equation, the force is not a polynomial function of the nodal position, which will cause great difficulty in the evaluation of our final equation. Therefore, we use a different model leading to a polynomial function of the nodal position, which is one of the highlights in this paper.

$$\mathbf{f}_s = k_s(r^2 - r_0^2) \mathbf{B}_s^T (\mathbf{x}_1 - \mathbf{x}_0) = k_s(\mathbf{x}_s^T \mathbf{B}_s^T \mathbf{B}_s \mathbf{x}_s - r_0^2) \mathbf{B}_s^T \mathbf{B}_s \mathbf{x}_s \quad (4)$$

where $k_s = \bar{k}_s / (2r_0^2)$. This time it is just a cubic function of the nodal position. When stretch or compression is small (That is the case of the deformation of a strand like object, $|r - r_0| \ll r_0$), Eq. (4) approximates Eq. (3). The deformation energy W_s can be obtained by the following integral:

$$W_s = \int_0^x \mathbf{f}_s d\mathbf{x}_s = \frac{k_s(\mathbf{x}_s^T \mathbf{B}_s^T \mathbf{B}_s \mathbf{x}_s - r_0^2)^2}{4} \quad (5)$$

1.2 Bend modeling

When the element bends, bend forces will be generated to resist this deformation. As the beam element is almost incompressible, we can consider that the length of the beam element is invariant. The bend angle must also be small (see Fig. 2), since the length of the beam element is small enough. We have the following approximate model:

$$|\mathbf{f}_b^0| = 2\bar{k}_b \alpha, \quad \mathbf{f}_b^1 = \mathbf{f}_b^2 = -\frac{\mathbf{f}_b^0}{2} \quad (6)$$

As the bend angle α is small enough, it can be approximately evaluated by

$$\alpha = 2a \sin\left(\frac{|\mathbf{x}_1 + \mathbf{x}_2 - 2\mathbf{x}_0|/2}{r_0}\right) \approx \frac{|\mathbf{x}_1 + \mathbf{x}_2 - 2\mathbf{x}_0|}{r_0} \quad (7)$$

Let

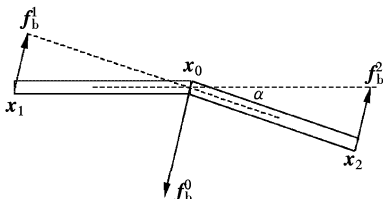


Fig. 2 A bend element generating elastic force

$$\mathbf{x}_b = \begin{Bmatrix} \mathbf{x}_0 \\ \mathbf{x}_1 \\ \mathbf{x}_2 \end{Bmatrix}, \quad \mathbf{f}_b = \begin{Bmatrix} \mathbf{f}_b^0 \\ \mathbf{f}_b^1 \\ \mathbf{f}_b^2 \end{Bmatrix}, \quad \mathbf{B}_b = [-2\mathbf{I} \quad \mathbf{I} \quad \mathbf{I}] \quad (8)$$

We obtain

$$\mathbf{f}_b = k_b \mathbf{B}_b^T \mathbf{B}_b \mathbf{x}_b \quad (9)$$

where $k_b = \bar{k}_b / r_0$. It is a linear function of a nodal position. Then the bend energy is a quadric function of the nodal position:

$$W_b = \frac{k_b \mathbf{x}_b^T \mathbf{B}_b^T \mathbf{B}_b \mathbf{x}_b}{2} \quad (10)$$

1.3 Elements integration

After obtaining the equation of the deformation energy of each element, we try to obtain the energy equation of the whole object by integrating all elements together. Let

$$\mathbf{x} = \begin{Bmatrix} \mathbf{x}_0 \\ \mathbf{x}_1 \\ \vdots \\ \mathbf{x}_{n-1} \end{Bmatrix}, \quad \mathbf{G}_s^i = [\mathbf{0} \dots \mathbf{0} \quad \mathbf{I}_{6 \times 6} \quad \mathbf{0} \dots \mathbf{0}], \quad \mathbf{G}_b^j = [\mathbf{0} \dots \mathbf{0} \quad \mathbf{I}_{9 \times 9} \quad \mathbf{0} \dots \mathbf{0}] \quad (11)$$

where $\mathbf{x}_0, \dots, \mathbf{x}_{n-1}$ are the position vectors of all nodes, \mathbf{G}_s^i and \mathbf{G}_b^j are the selection matrices for the i -th beam element and the j -th bend element, respectively. The matrix \mathbf{G}_s^i consists of n submatrices of 6×6 . Only the i -th submatrix is an identity matrix; the others are zero matrices. The structure of matrix \mathbf{G}_b^j is similar to that of \mathbf{G}_s^i , but its submatrix dimension is 9×9 . We obtain

$$W_e = \frac{k_s}{4} (\mathbf{x}^T \mathbf{A} \mathbf{x} - r_0^2)^2 + \frac{k_b}{2} \mathbf{x}^T \mathbf{T} \mathbf{x} \quad (12)$$

where

$$\mathbf{A} = \sum_{i=0}^{n-2} (\mathbf{G}_s^i)^T \mathbf{B}_s^T \mathbf{B}_s \mathbf{G}_s^i, \quad \mathbf{T} = \sum_{j=0}^{n-3} (\mathbf{G}_b^j)^T \mathbf{B}_b^T \mathbf{B}_b \mathbf{G}_b^j \quad (13)$$

1.4 Twist consideration

A thorough twist model is complicated and difficult to implement in a real-time simulation algorithm. So we develop an approximate model that can satisfy the basic clinical demands. The configuration of a beam element can be described by its nodal position and a coordinate frame of “directions” attached to the element (see Fig. 3). While one beam can move in its nodal position, it can also rotate round its axial, which causes twists between connected beams. We can map the directions of a local coordinate frame of one beam to its neighbor beam’s coordinate frame to calculate the twist angle at the connecting node ($\Delta\theta$ in Fig. 3 is the angle between the two x axes).

When there is a twist, there is torsion passing the connecting node:

$$T = k_t \Delta\theta \quad (14)$$

As a twist just changes $\Delta\theta$ and has nothing to do with the

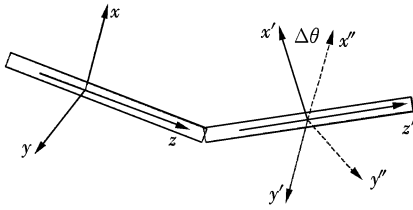


Fig. 3 The local coordinate frame (x, y, z) mapped to its neighbor's coordinate (x', y', z')

nodal position, we can separate a guide wire's deformation in shape from that of a twist. The torsion equilibrium for each beam of the guide wire can be established.

$$k_t(\Delta\theta_{i+1} - \Delta\theta_i) = T_i \quad (15)$$

where $\Delta\theta_{i+1}$ and $\Delta\theta_i$ are twist angles at the two nodes of the i -th beam element of the guide wire and T_i is the external torsion applied to that beam element. As $\Delta\theta_0$ is zero (Node 0 is the beginning of the beam chain and there is no twist at this node), we can calculate the twist angles one by one with Eq. (15). These angles represent a twist configuration of the guide wire.

1.5 Vascular structure representation

The vascular structure is originally represented by a 3-D description defined by a triangular mesh extracted from the CT data of a patient. This mesh just represents the inner surface of the artery wall. We try to extend this surface mesh to a tetrahedron mesh by converting each triangle element into a tetrahedron element. For each triangle element, we find its center point and move it for a given distance along the direction of the normal of the triangle to a point out of the artery. This point and the three vertexes of the triangle form a tetrahedron. The new point called the static node, which never moves, works as a home retractor trying to restore the triangle back to its initial position. This makes the artery seem to rest on the background of the soft tissue that tries to hold the artery in place. That is the case in the real human body. Because the new point's position is known and never changes, it does not introduce any additional computational complexity. With the tetrahedron mesh we can build an FEM model of the artery. As displacements of the artery remain quite small, a linear FEM model is appropriate for artery modeling, which remarkably simplifies the question:

$$W_a = \frac{1}{2} \mathbf{x}_a^T \mathbf{K} \mathbf{x}_a, \quad \mathbf{f}_a = \mathbf{K} \mathbf{x}_a \quad (16)$$

where W_a is the deformation energy of the artery, \mathbf{f}_a is the elastic force vector, \mathbf{K} is the stiffness matrix, and \mathbf{x}_a is the nodal displacement vector.

1.6 Guide wire's deformation simulation

According to the Newtonian law of motion the force equilibrium for each node of the guide wire can be established:

$$\mathbf{M} \frac{d^2 \mathbf{x}}{dt^2} + \mathbf{D} \frac{d\mathbf{x}}{dt} + \mathbf{f}(\mathbf{x}) = \mathbf{f}_{\text{ext}} \quad (17)$$

where \mathbf{M} is the mass matrix, \mathbf{D} is the damping matrix, $\mathbf{f}(\mathbf{x})$ is the elastic force, and \mathbf{f}_{ext} is the external force. Usually the ex-

ternal force includes two parts: the known external load and the contact force \mathbf{f}_c . The contact force on a guide wire node is in the direction of the normal of the contacted triangle of the artery and its magnitude is decided by $f_c = k_c d$, where d is the depth of the node penetrating into the artery wall and k_c the contact stiffness coefficient. In order to solve Eq. (17), two different forms applying Euler's method have been proposed to discretize time^[5,10]. However, the stability of these approaches largely depends on the selection of an appropriate time step. A small time step is necessary to lead to a stable solution which means a high computational cost, since we have to finish the update of the model within one time step. As a result, these kinds of methods are not suitable for real-time simulation. Consequently, we suggest a new method based on the process of potential energy dissipation in viscoelastic solid.

The potential energy of an elastic body includes two parts: the elastic deformation energy and the potential energy of external forces. In our case, this energy is a polynomial function of the nodal position. Considering (12), we have

$$W(\mathbf{x}) = W_e - \mathbf{f}_{\text{ext}}^T \mathbf{x} = \frac{k_s [\mathbf{x}^T \mathbf{A} \mathbf{x} - r_0^2]^2}{4} + \frac{k_b \mathbf{x}^T \mathbf{T} \mathbf{x} - \mathbf{f}_{\text{ext}}^T \mathbf{x}}{2} \quad (18)$$

The composite force vector applied to nodes can be obtained by the derivation of the potential energy with respect to the nodal position.

$$\mathbf{f}_{\text{co}} = -\nabla W(\mathbf{x}) = -\mathbf{f}(\mathbf{x}) + \mathbf{f}_{\text{ext}} \quad (19)$$

If the composite force is zero, the model is in a state of static equilibrium. If not zero, the model is in an unstable state and will deform to its final stable configuration of a state of static equilibrium. This deformation process will take some time depending on the viscosity of the model. If the model does not have any viscosity, the model will immediately fall to the final stable configuration without any delay. If it has some viscosity, the model will gradually deform to the final configuration and dissipate its potential energy step by step. We try to discretize this deformation process with a non-linear conjugate gradient method. Usually the conjugate method is used for the evaluation of the final stable configuration, but here we also use its middle results to simulate the whole deformation process. First we compute an energy gradient and decide on a displacement direction also known as the search direction. We can calculate this search direction by the following recursion^[11]:

$$\mathbf{P}_k = \begin{cases} -\mathbf{g}_k & k=1 \\ -\mathbf{g}_k + \beta \mathbf{P}_{k-1} & k>1 \end{cases}, \quad \beta = \frac{\|\mathbf{g}_k\|^2}{\|\mathbf{g}_{k-1}\|^2} \quad (20)$$

where \mathbf{g}_k and \mathbf{g}_{k-1} are the energy gradients at current time t_k and last time t_{k-1} , and \mathbf{P}_k and \mathbf{P}_{k-1} are the current and last search directions. Then

$$\mathbf{x}_{k+1} = \mathbf{x}_k + \lambda \mathbf{P}_k \quad (21)$$

where \mathbf{x}_k is the current known configuration at time t_k , \mathbf{x}_{k+1} is the next unknown configuration at time t_{k+1} , and λ is an unknown quantity for evaluation.

Substituting Eq. (21) into Eq. (18), we obtain

$$W(\lambda) = a_4 \lambda^4 + a_3 \lambda^3 + a_2 \lambda^2 + a_1 \lambda + a_0 \quad (22)$$

where

$$\begin{aligned}
 a_4 &= \frac{k_s (\mathbf{P}_k^T \mathbf{A} \mathbf{P}_k)^2}{4} \\
 a_3 &= \frac{k_s \mathbf{x}_k^T \mathbf{A} \mathbf{P}_k \mathbf{P}_k^T \mathbf{A} \mathbf{P}_k}{2} \\
 a_2 &= \frac{k_s \mathbf{x}_k^T \mathbf{A} (\mathbf{x}_k \mathbf{P}_k^T + 2 \mathbf{P}_k \mathbf{x}_k^T) \mathbf{A} \mathbf{P}_k + k_b \mathbf{P}_k^T \mathbf{T} \mathbf{P}_k}{2} \\
 a_1 &= k_s \mathbf{x}_k^T \mathbf{A} \mathbf{x}_k \mathbf{x}_k^T \mathbf{A} \mathbf{P}_k + k_b \mathbf{x}_k^T \mathbf{T} \mathbf{P}_k - \mathbf{f}_{\text{ext}}^T \mathbf{P}_k
 \end{aligned}$$

So the potential energy is a polynomial function of λ . We can find the minimal energy point by solving the following equation:

$$\frac{dW}{d\lambda} = 4a_4\lambda^3 + 3a_3\lambda^2 + 2a_2\lambda + a_1 = 0 \quad (23)$$

After obtaining λ , we can compute \mathbf{x}_{k+1} by Eq. (21).

Repeat this procedure till the final stable configuration is attained or approached. Because the conjugate method is non-conditionally convergent and stable, this iterated process must also work. As the model evolves to a configuration with minimal energy during each iteration, it is also an efficient iteration. That means the model will quickly converge to a stable configuration. Here, we assume that the process of each iteration takes the same period of time (time step τ) that characterizes the viscosity of the model. Experimental results show that a range from 1 to 10 ms of τ can result in a desirable simulation effect.

Analysis of the conjugate method shows that the middle results of the conjugate method are different from the results of the explicit or the semi-implicit Euler method^[10], but the final stable results of these methods are the same. Despite the difference in middle results, the new method's stability and high efficiency prove of high value in real-time simulation. In the case of real-time surgery simulation, stability and efficiency are more important than fidelity^[9]. So the significance of the method in real-time surgery simulation is considerable.

2 Results

Our method is tested on a guide wire inserted into an artificial tube and an artery segment reconstructed from the CT data of a patient. We also simulate the deformation of a guide wire deformed by gravity with our method.

A guide wire (composed of 20 beam elements, element length: 2 mm, element weight: 0.2 g, $k_b = 100$ N/m, $k_s = 10^{10}$ N/m³) with its left terminal fixed is deformed by gravity from its initial horizontal configuration to the final stable configuration (see Fig. 4). With our method using a time step of 1 ms we can simulate this process stably as well as efficiently. When the simulation is implemented with the explicit

method, we must use a time step as short as 1 μ s to keep the computation stable that leads to a high computational cost (see Tab. 1).

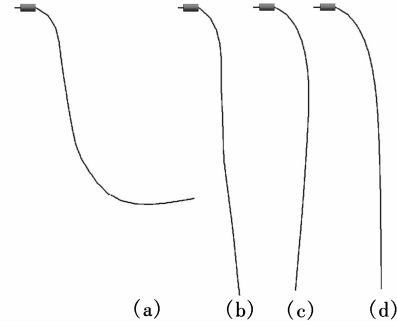


Fig. 4 Simulation of the deformation of a guide wire deformed by gravity. (a) $t=0.5$ s; (b) $t=1$ s; (c) $t=2$ s; $t=4$ s

Fig. 5 illustrates the simulation of a guide wire interacting with a tube segment composed of 1 160 triangles. The guide wire contains 20 beam elements and its parameters are $k_b = 10^5$ N/m and $k_s = 10^{12}$ N/m³. The top image represents the initial configuration. The bottom is the result of the deformation.



Fig. 5 A guide wire interacting with a tube segment

Fig. 6 illustrates the simulation of a guide wire inserted into a real human artery segment model of 5 472 elements extracted from a CT data set of a patient.

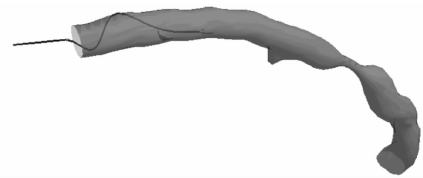


Fig. 6 Simulation of a guide wire inserted into a real human artery segment model

Based on the experiment shown in Fig. 4, some comparisons between our method and the explicit method are shown in Tab. 1.

Computational time in the table is the CPU time consumed in each method for the simulation of the deformation of a one-second period of the model.

Tab. 1 Comparison between our model and the other models

Method	Model's parameters	Time step/ms	Computational time/ms	Stability
Our method	20 beam elements $k_b = 100$ N/m	1	65	Non-conditional stable
	$k_s = 10^{10}$ N/m ³			
Explicit method	Element length: 2 mm Element weight: 0.2 g	10^{-3}	14 741	Conditional stable

3 Conclusion

We have presented the theory and implementation of a new method for the simulation of a guide wire passing through a vasculature. The model attempts to simulate the behavior of a guide wire efficiently as well as stably by introducing the conjugate gradient method to discretize the deformation of viscoelastic body. Experimental results show that the method improves simulation performance significantly in stability as well as efficiency. Despite the demonstrated advantages, there are still some researches needed in the future. The most urgent one might be to take twist action into full consideration, which is also the objective of our future research.

References

- [1] Lenoir J, Meseure P, Grisoni L, et al. A suture model for surgical simulation [C]//*Medical Simulation International Symposium*. Heidelberg: Springer, 2004: 105 – 113.
- [2] LeDuc M, Payandeh S, Dill J. Toward modeling of a suturing task [C]//*Graphics Interface'03 Conference*. Halifax: Canadian Computer-Human Communications Society, 2003: 265 – 272.
- [3] Konings M K, van de Kraats E, Alderliesten T, et al. Analytical guide wire motion algorithm for simulation of endovascular interventions [J]. *Medical and Biological Engineering and Computing*, 2003, **41**(6): 689 – 700.
- [4] Cotin S, Durez C, Lenoir J, et al. New approaches to catheter navigation for interventional radiology simulation [C]//*Medical Image Computing and Computer-Assisted Intervention*. Heidelberg: Springer, 2005: 534 – 542.
- [5] Guilloux V, Haigron P, Goksu C, et al. Simulation of guide-wire navigation in complex vascular structures [C]//*Proc of SPIE, Medical Imaging 2006: Visualization, Image-Guided Procedures and Display*. San Diego, 2006: 40 – 50.
- [6] Cao D Q, Liu D S, Charles H, et al. Three-dimensional nonlinear dynamics of slender structures: cosserat rod element approach [J]. *International Journal of Solids and Structures*, 2006, **43**(4): 760 – 783.
- [7] Pai Dinesh K. Strands: interactive simulation of thin solids using cosserat models [J]. *Computer Graphics Forum*, 2002, **21**(3): 347 – 352.
- [8] Kukuk M, Geiger B. A real-time deformable model for flexible instruments inserted into tubular structures [C]//*Medical Image Computing and Computer-Assisted Intervention*. Heidelberg: Springer, 2002: 331 – 338.
- [9] Bro-Nielsen M. Finite element modeling in surgery simulation [J]. *Proceedings of the IEEE*, 1998, **86**(3): 490 – 503.
- [10] Meier U, López O, Monserrat C, et al. Real-time deformable models for surgery simulation: a survey [J]. *Computer Methods and Programs in Biomedicine*, 2005, **77**(3): 183 – 197.
- [11] Powell M J D. Nonconvex minimization calculations and the conjugate gradient method [C]//*Lecture Notes in Mathematics*. Berlin: Springer-Verlag, 1984: 122 – 141.

一种实时模拟血管中引导线变形的有限元模型

张秋葵¹ Pascal Haigron² 罗立民¹ 舒华忠¹

(¹东南大学影像科学与技术试验室, 南京 210096)

(²雷恩第一大学信号与图像处理实验室, 法国雷恩 35042)

摘要:为了实时仿真微创介入手术过程中引导线在外力作用下的变形,提出了一种适合于描述纤细物体力学特性的模型.通过对引导线的仿真,医生可以在术前预演手术,并选择最佳的手术方案.模型采用多体结构离散化引导线,根据弹性理论推导出引导线的弹性能是节点位移的多项式函数,病人的血管四面体网格模型可从血管的三角面网格模型拓广得到,并将共轭梯度法能量下降的过程应用于引导线变形过程的模拟.实验结果表明:由于模型的弹性能和节点位移呈多项式函数关系,共轭梯度法的求解得到了有效的简化,模型的效率有显著提高.与目前广泛采用的显式计算模型相比不仅稳定且更快速.模型可应用于血管中引导线变形的实时仿真.

关键词:变形模型;有限元;实时仿真;引导线

中图分类号:TP391